Photochemistry in a 3D metal-organic-framework (MOF) : Monitoring Intermediates and Reactivity of the *fac*- to *mer*- photoisomerization of Re(diimine)$(CO)_3Cl$ incorporated in a MOF.

Timothy L. Easun, Junhua Jia, James A. Calladine, Danielle L. Blackmore, Christopher S. Stapleton, Khuong Q. Vuong, Neil R. Champness* and Michael W. George*

School of Chemistry, University of Nottingham, University Park, Nottingham NG7 2RD, United Kingdom. Corresponding authors: neil.champness@nottingham,ac.uk, +44 (0)115 9513505; mike.george@nottingham.ac.uk, +44 (0)115 9513512

Abstract

The mechanism and intermediates in the UV-light initiated ligand rearrangement of *fac*-Re(diimine)$(CO)_3Cl$ to form the *mer*-isomer, when incorporated into a 3D metal-organic framework (MOF), have been investigated. The structure hosting the Re dimine complex is a 3D-network with the formula $\{Mn(DMF)_2[LRe(CO)_3Cl]\}_\infty$ (**ReMn**), where the diimine ligand L, 2,2'-bipyridine-5,5'-dicarboxylate, acts as a strut of the MOF. The incorporation of **ReMn** in a KBr disc allows the spatial distribution of the *mer*-isomer photoproduct in the disc to be mapped and spectroscopically characterised by both FTIR and Raman microscopy. Photoisomerization has been monitored by IR spectroscopy and proceeds via dissociation of a CO to form more than one dicarbonyl intermediate. The dicarbonyl species are stable in the solid-state at 200 K. The photodissociated CO ligand appears to be trapped within the crystal lattice and, on warming above 200 K, readily recombines with the dicarbonyl intermediates to form both the *fac*-Re(diimine)$(CO)_3Cl$ starting material and the *mer*-Re(diimine)$(CO)_3Cl$ photoproduct. Experiments over a range of temperatures (265-285 K) allow estimates of the activation enthalpy of recombination for each process of *ca*. 16 (± 6) $kJmol^{-1}$ (*mer*-formation) and 23 (± 4) $kJmol^{-1}$ (*fac*-formation) within the MOF framework. We have compared the photochemistry of the **ReMn** MOF with a related alkane soluble Re(dnb)$(CO)_3Cl$ complex (dnb = 4,4'-dinonyl-2,2'-bipyridine). Time-resolved IR measurements clearly show that in alkane solution, the photoinduced dicarbonyl species again recombines with CO to both reform the *fac*-isomer starting material and to form the *mer*-isomer photoproduct. DFT calculations of the possible dicarbonyl species aids the assignment of the experimental data in that the ν(CO) IR bands of the CO loss intermediate are, as expected, shifted to lower energy when the metal is bound to DMF rather than to an alkane and both solution data and calculations suggest that the ν(CO) band positions in the photo-produced dicarbonyl intermediates of **ReMn** are consistent with DMF binding.

Introduction

The photochemistry of Re-diimine complexes are of great interest for a range of applications including photocatalysts for CO_2 reduction,[1] as photoluminescent probes for studying DNA damage,[2] in electroluminescent devices[3] and as luminescent components for supramolecular photochemistry.[4] *fac*-Re(bpy)$(CO)_3$Cl (bpy = 2,2'-bipyridine) has been extensively studied, but synthesis of the *mer*-isomer was only reported in 2007, following photochemically-induced CO loss in tetrahydrofuran (THF) solution under CO. The *mer*-isomer has been shown to be synthetically useful in producing novel dicarbonyls[5] and the solution phase photochemistry of its formation has been studied by fast spectroscopic techniques.[6]

The incorporation of photoactive metal centres into metal-organic frameworks (MOFs) is a rapidly developing area building on the applications of MOFs in magnetism,[7] gas-storage,[8] drug delivery,[9] catalysis[10] and photochemistry,[11] with studies demonstrating the ability of MOFs to stabilise unusual intermediates, taking advantage of the unusual environment and rigidity of the frameworks. Indeed, MOFs and related coordination cages provide fascinating rigid hosts that can be considered as structured matrices for performing either chemical[12] or photochemical reactions.[13,14]

We previously reported the *fac*- to *mer*-isomerism of the Re(diimine)$(CO)_3$Cl unit directly incorporated into the framework of a MOF.[14] This **ReMn** MOF contains the Re(2,2'-bipyridine-5,5'-dicarboxylate)$(CO)_3$Cl unit as the linker and manganese at the nodes, forming a 3D network structure. The nature of the short-lived (ps-ns) excited states of this *fac*-isomer and the product formation (*mer*-isomer) were reported with the latter being characterised by both FTIR and X-ray crystallography.

In this paper we investigate the unsaturated *intermediates* involved in the photoisomerisation. A comparison with time-resolved IR studies of Re(dnb)$(CO)_3$Cl (dnb = 4,4'-dinonyl-2,2'-bipyridine) in alkane solvents in the presence and absence of DMF is reported and a computational study of the possible intermediates is discussed.

Results and Discussion

The ground-state crystal structure of $\{Mn(DMF)_2[LRe(CO)_3Cl]\}_\infty$ (**ReMn**), L = 2,2'-bipyridine-5,5'-dicarboxylate, which we first reported in 2010[14] is shown in Figure 1. The extended network is stable in air and even at 100°C for greater than two days. The MOF has been designed such that the local structural changes around the Re(I) centre are unlikely to influence the overall framework structure. The infrared spectrum of **ReMn** recorded in a KBr disc displays ν(CO) bands at 2015, 1917 and 1882 cm^{-1} consistent with the *fac*-isomer of the Re(diimine)$(CO)_3$Cl moiety. The Raman spectrum in the same conditions displays bands at 1606, 1592, 1495, 1412, 1360 and 1308 cm^{-1}.

We previously investigated[14] the effect of UV photolysis of **ReMn** in a KBr disc using FTIR imaging. Here we compare the FTIR and Raman maps of the separate discs both before and after UV photolysis at 275 K. The FTIR spectra are particularly definitive in the ν(CO) spectral region and the Raman spectra afford further information on the backbone of the framework. The results are displayed in Figure 2. Visually, the yellow discs darken in the centre where irradiation was performed (the outer region of the discs were masked by the cell in which they were mounted). In both the FTIR and Raman spectra, notable changes are observed in this region of the discs. The IR difference spectrum obtained after 8 hours photolysis is shown in Figure 2(d). The parent ν(CO) bands are clearly bleached and several new absorptions can be seen. The FTIR experiments are consistent with our previous report of *fac*- to *mer*- isomerisation within the MOF framework and new ν(CO) bands are produced at 2043, 1925 and 1868 cm^{-1} due to the *mer*-isomer.[13] The depletion in the *fac* ν(CO)

band at 2015 cm^{-1} following 20 hours photolysis suggest 10% of the starting *fac*-isomer is photolysed to the *mer*-isomer in these experiments. Plotting the ratio of the *mer*-isomer IR band at 2043 cm^{-1} to the *fac*-isomer band at 2015 cm^{-1} affords the FTIR image of the whole KBr disc shown in Figure 2(b), in which the formation of the *mer*-isomer in the central region of the disc can clearly be observed, in good agreement with the visual observation of the KBr disc.

We have also investigated the formation of the *mer*- isomer using Raman spectroscopy. The ground state Raman spectrum (Figure 2(f)) shows overlapping bands in the region around 1600 cm^{-1} which correspond to DMF bound to the Mn nodes and to the carboxylate groups of the MOF linkers. There are a series of lower energy Raman bands (1500–1300 cm^{-1}) which correspond to ring modes of the bipyridine ligand. All of these Raman features probe the subtle changes of framework structure on photolysis and isomerisation rather than the direct probe of metal coordination afforded by the FTIR spectra. The Raman spectral changes are shown as a difference spectrum in Figure 2(f); formation of the *mer*-isomer being accompanied by a decrease in the parent band intensity around 1600 and 1500 cm^{-1} and appearance of product bands at lower energy. Plotting the percentage of the *mer*-isomer against that of the *fac*-isomer, affords an image showing the distribution of the *mer*-isomer in the central region of the disc (Figure 2(e)) in much the same way as the FTIR spectral mapping experiment. This demonstrates the sensitivity of both the Raman technique and of the framework to indirect structural alterations, i.e. the exchange of CO and Cl ligands around the Re centre measurably affects the vibrational manifold of the MOF framework. This will be particularly important in future studies of MOFs which do not contain functional groups readily characterisable by infrared spectroscopy.

Determination of the pathway of the *fac*- to *mer*-isomerisation process in ReMn.

The *fac*- to *mer*-isomerisation in the **ReMn** MOF at 275 K proceeds via photodissociation of a carbonyl ligand to form two primary dicarbonyl intermediate(s) with ν(CO) bands at 1893, 1855, 1813 and 1794 cm^{-1}, identified by band fitting of the FTIR difference spectra using Lorentzian line-shapes.[14,15,16] There are several possible CO–loss intermediates, which can be considered as either incorporating a vacant metal site or involving coordination of an alternative ligand (see DFT calculations below and Figure 3). In the latter case there are four possible octahedral geometries for $[Re(bpy)L(CO)_2Cl]$ determined by the position of both the chloride and L (axial or equatorial) which correspond to (a) ax-Cl, eq-L; (b) ax-Cl, ax-L; (c) eq-Cl, eq-L and (d) eq-Cl, ax-L. In the case of the vacant metal site, experiments by Ishitani *et al.* have shown that the coordinatively unsaturated intermediate in *solution* only survives on the early picosecond timescale before reacting with solvent.[6]

The nature of our experimentally identified solid-state dicarbonyl intermediate(s) was unclear so we investigated the effect of temperature on the reactivity and band positions of the species observed in the FTIR spectra after photolysis. In a series of experiments the CO loss intermediate(s) were produced by ~20 hours photolysis of the MOF in KBr discs at 200 K. Each disc was then warmed to a specific temperature and the thermal behavior of the photoproducts was monitored using FTIR spectroscopy. On warming to 275 K, the bands assigned to the CO loss products decayed and the bands of the *fac*- and *mer*-isomers increased in intensity. The recovery of the *fac*-isomer (k_{obs} = 8.6 (± 3.0) x 10^{-5} s^{-1}) and the formation of the *mer*-isomer (k_{obs} = 6.1 (± 1.3) x 10^{-4} s^{-1}) were each fitted to a mono-exponential process. The decrease in intensity of the dicarbonyl bands can be fitted to a bi-exponential decay which correlates with the growth of *mer*- and *fac*- isomers respectively (k_{obs} = 7.4 (± 0.6) x 10^{-4} and 8.2 (± 0.5) x 10^{-5} s^{-1}).

More careful inspection of the spectroscopic data using band fitting reveals the presence of a ν(CO) band which decays quickly at 1813 cm^{-1} and one which decays more slowly at 1794 cm^{-1}. The different kinetic behavior of the two CO loss intermediates manifests itself by the later time FTIR spectra being dominated by the lower energy band in this region.[†] The assignment of these two dicarbonyl intermediates can be tentatively made based on previously reported[15] solution FTIR spectra of [Re(bpy)$(CO)_2(CH_3CN)$Cl], with the 1893 and 1813 cm^{-1} bands being due to the [Re(bpy)$(CO)_2$Cl] with the chloride in the equatorial position and the lower energy 1855 and 1794 cm^{-1} pair corresponding to [Re(bpy)$(CO)_2$Cl] with the chloride in the axial position. Further evidence for these assignments is that the former decays at the same rate as the *mer*-isomer grows in and the latter matches the formation of the *fac*-isomer, both of which are consistent with addition of CO to the available coordination site without need for ligand rearrangement. Once formed, the *mer*-isomer is stable in the solid state at room temperature.

We have examined the formation of the *mer*-isomer further by determining the kinetics of dicarbonyl decay and tricarbonyl growth at specific temperatures between 260 and 285 K. Plotting these data on an Arrhenius plot (Figure 4) allows the estimation of E_a for formation of the *mer*- (16 (± 6) $kJmol^{-1}$) and *fac*-isomer (23 (± 4) $kJmol^{-1}$) from the dicarbonyl species. The slightly lower E_a for *mer*-formation is consistent with the observed faster decay (described above) at 275 K of the bands associated with the dicarbonyl species corresponding to that with the chloride ligand in the equatorial position, i.e. predisposed towards *mer*-formation (although it should be noted that these activation energies are very similar and within error).

In further experiments we irradiated MOF-containing KBr discs at low temperature both under vacuum and under high pressure of N_2 (2000 psi) and obtained very similar results with no evidence for formation of a new dinitrogen complex. During both experiments the formation of free CO was evident in the IR spectra at ~2130 cm^{-1}. These results suggest that the photodissociated CO could not easily be removed from the crystalline framework and is essentially trapped within the MOF matrix.

Solvent coordinated Intermediates in the Isomerization Process.

The crystal structure of **ReMn** shows the presence of DMF bound to the Mn nodes in the MOF. One question that arises is whether the dicarbonyl intermediates are naked or stabilized by coordination of a neighboring DMF molecule. The presence of two distinct pairs of bands for the dicarbonyl intermediates suggests that the movement of chloride is not occurring on the timescale of the experiment, possibly indicating the presence of DMF binding and the lack of a truly vacant site. The coordination of solvents to reactive intermediates produced via photochemical dissociation of CO from metal carbonyls is well established even with weakly coordinating solvents such as alkanes. With these weakly coordinating ligands CO loss can produce long-lived organometallic alkane complexes which can be characterized by IR and NMR spectroscopies.[17] With the strongly coordinating DMF ligand in the **ReMn** MOF the similarity of ν(CO) band position of the dicarbonyls obtained after photolysis with those reported[15] for [Re(bpy)$(CO)_2(CH_3CN)$Cl] suggests that DMF is coordinated since electron-donating solvent coordination will increase the electron density on the metal centre, more than with weakly coordinating solvents such as alkanes, and shift the ν(CO) bands further to lower wavenumber (Table 1). Fast time-resolved IR (TRIR) spectroscopy has characterized the dissociative isomerisation of [Mn(^{i}Pr-DAB)$(CO)_3$Br] (^{i}Pr-DAB = N,N'-diisopropyl-1,4-diazabutadiene) and again similar shifts in ν(CO) bands were reported on formation of the dicarbonyl species with solvent coordinated to the vacant site.[16]

More definitive evidence could be obtained by characterizing [Re(bpy)(CO)$_2$Cl] in weakly coordinating alkane solvents to measure the smaller shifts one would predict. Unfortunately, the *fac*-[Re(bpy)(CO)$_3$Cl] precursor is insoluble in alkane solvents and we have therefore synthesized an alkyl substituted analogue, *fac*-[Re(dnb)(CO)$_3$Cl] (dnb = 4,4'-dinonyl-2,2'-dipyridyl) which dissolves in cyclopentane. Irradiation (266 nm) of *fac*-[Re(dnb)(CO)$_3$Cl] in cyclopentane generates a dicarbonyl species with ν(CO) bands centered around 1914 and 1828 cm^{-1} which subsequently react with CO to form *fac*- and *mer*-[Re(dnb)(CO)$_3$Cl] (Figure 5) on a timescale of ~1 second. Doping the cyclopentane with DMF (v/v 10%) results in the formation of ν(CO) bands due to [Re(dnb)(CO)$_2$Cl] centered around 1900 and 1810 cm^{-1} (Table 1). These bands are *ca*. 16 cm^{-1} to lower energy than the dicarbonyl species observed in cyclopentane alone, while the parent absorptions shift less, by 0-10 cm^{-1} (likely indicative of a weak preferential solvation effect). Furthermore, the dicarbonyl species were long-lived in DMF (>1hr) and these results suggest that the intermediate in this case is better formulated as [Re(dnb)(CO)$_2$(DMF)Cl].

Comparing the solution results with those obtained for the **ReMn** MOF show that the shift in ν(CO) bands in the solid state experiment upon photolysis is consistent with DMF being bound to the metal centre following photodissociation of CO. This is also consistent with the long-lived nature of these species (minutes – hours) and the slow recombination to form parent and *mer*-isomers. Once the loss of dicarbonyl intermediates is complete no further spectral changes are observed either in the solid or in the solution experiments on their respective timescales; days for the solid-state and minutes for the solution phase, the latter then being subject to diffusion of the photoproduct away from the region being monitored.

DFT Modelling of Intermediates in the Photodissociation Process.

We have also performed some DFT calculations to provide more evidence for the identity of the possible intermediates involved in photodissociation. Table 1 shows the calculated ν(CO) IR band positions of *fac*-[Re(bpy)(CO)$_3$Cl]; *mer*-[Re(bpy)(CO)$_3$Cl], [Re(bpy)(CO)$_2$Cl] and [Re(bpy)L(CO)$_2$Cl] (L = CH_4 or a DMF molecule). As described above, there are four possible octahedral geometries for [Re(bpy)L(CO)$_2$Cl] determined by the position of both the chloride and L (axial or equatorial): (a) ax-Cl, eq-L; (b) ax-Cl, ax-L; (c) eq-Cl, eq-L and (d) eq-Cl, ax-L (Figure 3). In the DFT calculation with a vacant site only one minimized geometry was obtained, (e), significantly distorted from octahedral. The calculated ν(CO) IR band positions are in the order [Re(bpy)(CO)$_2$Cl] > [Re(bpy)(CH_4)(CO)$_2$Cl] > [Re(bpy)(DMF)(CO)$_2$Cl], consistent with the experimental observations in cyclopentane and in cyclopentane doped with 10% DMF in which the shift is *ca*. 16 cm^{-1} to lower energy. Furthermore, in both the [Re(bpy)(CH_4)(CO)$_2$Cl] and [Re(bpy)(DMF)(CO)$_2$Cl] dicarbonyl species the calculated ν(CO) bands for the isomers with axial chloride are lower in energy than for the corresponding structures with equatorial chloride.[‡] These observations further support the tentative assignment for **ReMn** above of the lower energy pair of ν(CO) dicarbonyl bands to an intermediate in which chloride is axial, which goes on to form the *fac*-isomer, and the assignment of the higher energy pair of ν(CO) dicarbonyl bands to an intermediate in which chloride is equatorial, which goes on to form the *mer*-isomer (as monitored by the kinetics).

Conclusions

The use of both FTIR and Raman mapping has demonstrated the utility of these techniques in spatially and spectrally identifying the *mer*-isomer product of the photolysis of **ReMn** in a KBr disc. We have used a combination of variable temperature experiments, photochemistry and FTIR spectroscopy to identify the presence of two dicarbonyl intermediates formed during photolysis. We

have measured the rates of formation of the *fac*- and *mer* isomers of **ReMn** from their respective dicarbonyl precursors and estimated E_a for these processes. The photolysis of [Re(dnb)$(CO)_3$Cl] in cyclopentane as a model has been used to investigate the nature of the reactive intermediates in the MOF by performing fast TRIR measurements in the presence and absence of DMF. These results were combined with DFT calculations to indicate that the dicarbonyl ν(CO) bands of the **ReMn** photoproduced intermediates are more consistent with the presence of bound DMF than the presence of a vacant site. The assignment of one intermediate to a dicarbonyl species with axial chloride (which forms the *fac*-isomer on CO addition) and the other intermediate to a dicarbonyl species with equatorial chloride (which forms the *mer*-isomer on CO addition) is consistent with the existing solution-phase literature, the matching of the dicarbonyl decay kinetics to the corresponding isomer formation on CO recombination and the computationally calculated differences in ν(CO) band positions for this family of reactive species.

Materials and Methods

Rhenium pentacarbonyl chloride, 5,5'-dimethyl-2,2'-dipyridyl and 4,4'-dinonyl-2,2'-dipyridyl were purchased from SIGMA-Aldrich and used without further treatment. **ReMn** was synthesised as previously described.[14]

Preparation of [Re(dnb)$(CO)_3$Cl], Re($C_{31}H_{44}N_2O_3Cl$): The synthetic procedure used was adapted from that reported in the literature to form the unsubstituted 2,2'-bipyridine complex. [$ReCl(CO)_5$] (0.724 g, 2.00 mmol) and 4,4'-$(C_9H_{19})_2$-2,2'-bpy (0.818 g, 2.00 mmol) were dissolved in toluene (120 ml) and heated at reflux under an atmosphere of dry argon gas for four hours. The resulting yellow solution was cooled to room temperature and the solvent evaporated to yield a bright yellow solid. The resulting crude product was recrystallised from hot methanol to yield a bright yellow microcrystalline solid in two crops.

Yield: 1.17 g, 81.9 % Elemental analysis: Calculated for {$ReC_{31}H_{44}N_2O_3Cl$}: C, 52.12; H, 6.21; N, 3.92 %. Found: C, 52.07; H, 6.09; N, 3.99 %. ^{1}H NMR ($CDCl_3$, 300 MHz): δ 8.89 (d, ^3J = 5.7 Hz, 2H, H^6), 7.94 (d, ^4J = 1.3 Hz, 2H, H^3), 7.32 (dd, ^3J = 5.7 Hz, ^4J = 1.3 Hz, 2H, H^5), 2.79 (t, ^3J = 7.9 Hz, 4H, ArC**H**$_2$), 1.71 (m, 4H, ArCH_2C**H**$_2$), 1.43-126 (m, 24H, C**H**$_2$), 0.88 (apparent t, ^3J = 7.0 Hz, 6H, C**H**$_3$) ppm. ^{13}C NMR ($CDCl_3$, 75 MHz): δ 197.4 (aq **C**O), 190.1 (ax **C**O), 156.0, 155.7, 152.8, 127.2, 123.1, 35.9, 32.0, 30.4, 29.6, 29.5, 22.8, 14.2 ppm.

Instrumentation

The instrumentation used to record the low-temperature KBr disc spectra has previously been described elsewhere.[19] Briefly, each KBr disc was cut to fit a copper cell with CaF_2 windows. The cell was sealed, purged with N_2 gas, evacuated, attached to a cold finger inside a vacuum shroud, and cooled to 200 K. Photolysis was achieved using a Philips HPK medium pressure 125 W mercury arc lamp and infrared spectra were recorded on a Thermo Nicolet Avatar 360 spectrometer (with 2 cm^{-1} resolution). Infrared mapping was performed using a Thermo Nicolet Continuüm XL Infrared Microscope with 15X magnification. Raman mapping was performed using a Horiba Jobin Yvon LabRAM HR Raman microscope with 50 X magnification and a 785 nm laser.

Point-by-point time-resolved IR spectra were recorded on apparatus which has been previously described elsewhere.[20] Briefly however, a pulsed Nd:YAG laser (Spectra Physics Quanta Ray GCR 12; 266 nm) is used to initiate the reaction and the change in IR absorbance with time, at a particular frequency is measured by an IR diode laser (Mutek MDS 1100). Kinetic measurements on a

timescale longer than 1 ms (the roll off time of the detector) were achieved by DC coupling the detector output to the amplifier. A solution IR cell (Harrick) with CaF_2 windows was fitted with customized Teflon spacers in order to limit diffusion of the photolysed sample out of the probe beam. Samples were prepared using standard Schlenk techniques under inert atmosphere. Fresh solution was used on each laser shot.

DFT Calculations

Density Functional calculations were performed using the Gaussian 03 program at the B3LYP level of theory.[18] The effective core potential, LANL2DZ was used on Re, and the 6-31G(d) basis set was used on the other atoms. Frequency calculations were performed on the geometry optimised structures.

Acknowledgements

We thank EPSRC and the University of Nottingham for financial support. MWG and NRC gratefully acknowledge receipt of Royal Society Wolfson Merit Awards.

Notes and references

† We were not able to deconvolute satisfactorily the kinetics of the high frequency CO loss bands due to the heavy overlap in this region.

‡ There is one minor exception whereby the lower energy ν(CO) band of $[Re(bpy)(CO)_2Cl]$ + DMF-1 is calculated to be at 1955 cm^{-1} but the lower energy band of $[Re(bpy)(CO)_2Cl]$ + DMF-3 is calculated to be 4 wavenumbers lower, at 1951 cm^{-1}.

1. (a) Morimoto, T.; Nakajima, T.; Sawa, S.; Nakanishi, R.; Imori, D.; Ishitani, O. *J. Am. Chem. Soc.*, **2013**, *135*, 16825–16828. (b) Doherty, M.D.; Grills, D.C.; Muckerman, J.T.; Polyansky, D.E.; Fujita, E. *Coord. Chem. Rev.*, **2010**, *254*, 2472–2482. (c) Coleman, A.; Brennan, C.; Vos, J.G.; Pryce, M.T. *Coord. Chem. Rev.*, **2008**, *252*, 2585–2595.
2. (a) Smith, J.A.; George, M.W.; Kelly, J.M. *Coord. Chem. Rev.*, **2011**, *255*, 2666–2675. (b) Cao, Q.; Creely, C.M.; Davies, E.S.; Dyer, J.; Easun, T.L.; Grills, D.C.; McGovern, D.A.; McMaster, J.; Pitchford, J.; Smith, J.A.; Sun, X.–Z.; Kelly, J.M.; George, M.W. *Photochem. Photobiol. Sci.*, **2011**, *10*, 1355–1364. (c) Butler, J.M.; George, M.W.; Schoonover, J.R.; Dattelbaum, D.M.; Meyer, T.J. *Coord. Chem. Rev.*, **2007**, *251*, 492–514; Metcalfe C.; Thomas, J.A. *Chem. Soc. Rev.*, **2003**, *32*, 214–224.
3. Si, Z.; Li, J.; Li, B.; Zhao, F.; Liu, S.; Li, W. *Inorg. Chem.*, **2007**, *46*, 6155–6163.
4. (a) Takeda, H.; Koike, K.; Morimoto, T.; Inumaru, H.; Ishitani, O. *Adv. Inorg. Chem.*, **2011**, *63*, 137–186. (b) Kirgan, R.A.; Sullivan B.P.; Rillema, D.P.; *Top. Curr. Chem.*, **2007**, *281*, 45–100. (c) Lees, A.J.; Sun, S.S. *Coord. Chem. Rev.*, **2002**, *230*, 171–192.
5. Sato, S.; Morimoto, T.; Ishitani, O. *Inorg. Chem.*, **2007**, *46*, 9051–9053.
6. Sato, S.; Matubara, Y.; Koike, K.; Falkenstrçm, M.; Katayama, T.; Ishibashi, Y.; Miyasaka, H.; Taniguchi, S.; Chosrowjan, H.; Mataga, N.; Fukazawa, N.; Koshihara, S.; Onda, K.; Ishitani, O. *Chem. Eur. J.*, **2012**, *18*, 15722–15734.
7. (a) Ouellette, W.; Prosvirin, A.V.; Whitenack, K.; Dunbar, K.R.; Zubieta, J. *Angew. Chem. Int. Ed.*, **2009**, *48*, 2140–2143. (b) Zhang, X.-M.; Hao, Z.-M.; Zhang, W.-X.; Chen, X.-M. *Angew. Chem. Int. Ed.* **2007**, *46*, 3456–3459. (c) Kurmoo, M. *Chem. Soc. Rev.*, **2009**, *38*, 1353–1379.
8. (a) Lin, X.; Blake, A.J.; Wilson, C.; Sun, X.; Champness, N.R.; George, M.W.; Hubberstey, P.; Mokaya, R.; Schröder, M. *J. Am. Chem. Soc.*, **2006***, 128,* 10745-10753. (b) Yang, S.; Lin, X.; Blake,

A.J.; Walker, G.S.; Hubberstey, P.; Champness, N.R.; Schröder, M. *Nature Chemistry*, **2009**, *1*, 487-493. (c) Tan, C.; Yang, S.; Lin, X.; Blake, A.J.; Lewis W.; Champness, N.R.; Schröder, M. *Chem. Commun.*, **2011**, *47*, 4487-4489 (d) Yan, Y.; Lin, X.; Yang, S.; Blake, A.J.; Dailly, A.; Champness, N.R.; Hubberstey, P.; Schröder, M. *Chem. Commun.*, **2009**, 1025-1027. (e) Farha, O.K.; Yazaydın, A.Ö.; Eryazici, I.; Malliakas, C.D.; Hauser, B.G.; Kanatzidis, M.G.; Nguyen, S.T.; Snurr, R.Q.; Hupp, J.T. *Nature Chem.,* **2010**, *2*, 944–948. (f) Lyndon, R.; Konstas, K.; Ladewig, B.P.; Southon, P.D.; Kepert, C.J.; Hill, M.R. *Angew. Chem. Int. Ed.* **2013**, *52*, 3695–3698. (g) Brown, J.W.; Henderson, B.L.; Kiesz, M.D.; Whalley, A.C.; Morris, W.; Grunder, S.; Deng, H.; Furukawa, H.; Zink, J.I.; Stoddart, J.F.; Yaghi, O.M. *Chem. Sci.*, **2013**, *4*, 2858–2864.

9. Horcajada, P.; Serre, C.; Maurin, G.; Ramsahye, N.A.; Balas, F.; Vallet-Regí, M.; Sebban, M.; Taulelle, F.; Férey, G. *J. Am. Chem. Soc.*, **2008**, *130*, 6774–6780.
10. (a) Shultz, A.M. ; Farha, O.K. ; Hupp, J.T. ; Nguyen, S.T. ; *J. Am. Chem. Soc.* **2009**, *131*, 4204–4205. (b) Hwang, Y.K. ; Hong, D.-Y. ; Chang, J.-S. ; Jhung, S.H. ; Seo, Y.-K. ; Kim, J. ; Vimont, A. ; Daturi, M.; Serre, C.; Férey, G. *Angew. Chem. Int. Ed.* **2008**, *47*, 4144–4148. (c) Fang, Q.-R. Yuan, D.-Q. ; Sculley, J. ; Li, J.-R.; Han, Z.-B. ; Zhou, H.-C. *Inorg.Chem.*, **2010**, *49*, 11637-11642. (d) Xie, Z. ; Wang, C. ; deKrafft, K.E.; Lin, W. *J. Am. Chem. Soc.*, **2011**, *133*, 2056-2059.
11. (a) Lan, A.; Li, K.; Wu, H.; Olson, D.H.; Emge, T.J.; Ki, W.; Hong, M.; Li, J. *Angew. Chem. Int. Ed.* **2009**, *48*, 2334–2338. (b) Chen, B.; Wang, L.; Xiao, Y.; Fronczek, F.R.; Xue, M.; Cui, Y.; Qian, G. *Angew. Chem. Int. Ed.* **2009**, *48*, 500–503. (c) Chandler, B.D.; Yu, J.O.; Cramb, D.T.; Shimizu, G.K.H. *Chem. Mater.*, **2007**, *19*, 4467–4473. (d) Modrow, A.; Zargarani, D.; Herges, R.; Stock, N. *Dalton Trans.*, **2011**, *40*, 4217–4222. (e) Takashima, Y.; Furukawa S.; Kitigawa, S. *CrystEngComm*, **2011**, *13*, 3360-3363. (f) Takashima, Y.; Martinez Martinez, V.; Furukawa, S.; Kondo, M.; Shimomura, S.; Uehara, H.; Nakahama, M.; Sugimoto, K.; Kitigawa, S. *Nature Comm.*, **2011**, *2*, 168. (g) Lee, C.Y.; Farha, O.K.; Hong, B.J.; Sarjeant, A.A.; Nguyen, S.T.; Hupp, J.T. *J. Am. Chem. Soc*., **2011**, *133*, 15858–15861. (h) Fateeva, A.; Chater, P.A.; Ireland, C.P.; Tahir, A.A.; Khimyak, Y.Z.; Wiper, P.V.; Darwent, J.R.; Rosseinsky, M.J. *Angew. Chem. Int. Ed*., **2012**, *51*, 7440–7444. (i) Wang, C.; Lin, W. *J. Am. Chem. Soc.*, **2011**, *133*, 4232–4235.
12. (a) Brozek, C.K.; Dincă, M.; *Chem. Sci*., **2012**, *3*, 2110-2113. (b) Haneda, T.; Kawano, M.; Kawamichi, T.; Fujita, M. *J. Am. Chem. Soc*., **2008**, *130*, 1578-1579. (c) Kawamichi, T.; Haneda, T.; Kawano, M.; Fujita, M. *Nature*, **2009**, *461*, 633-635.
13. (a) Xie, Z.; Ma, L.; deKrafft, K. E.; Jin, A.; Lin, W. *J. Am. Chem. Soc*. **2010**, *132*, 922–923; (b) Wang, C.; Wang, J-L.; Lin, W. *J. Am. Chem. Soc.*, **2012**, *134*, 19895–19908. (c) Kaye, S.S.; Long, J.R. *J. Am. Chem. Soc*., **2008**, *130*, 806-807. (d) Kawano, M.; Kobayashi, Y.; Ozeki, T.; Fujita, M. *J. Am. Chem. Soc*., **2006**, *128*, 6558-6559. (e) Easun, T.L.; Jia, J.; Reade, T.J.; Sun, X-Z.; Davies, E.S.; Blake, A.J.; George, M.W.; Champness, N.R. *Chem. Sci.*, **2014**, *5*, 539-544.
14. Blake, A. J.; Champness, N.R.; Easun, T.L.; Allan, D.R.; Nowell, H.; George, M.W.; Jia, J.; Sun, X.-Z. *Nature Chem*., **2010**, *2*, 688-694.
15. (a) Kleverlaan, C.J.; Hartl, F.; Stufkens, D.J. *J. Photochem. Photobiol. A*, **1997**, *103*, 231-237. (b) Kleverlaan, C.J.; Hartl F.; Stufkens, D.J. *J. Organomet. Chem.*, **1998**, *561*, 57-65. (c) Sato, S.; Sekine, A.; Ohashi, Y.; Ishitani, O.; Blanco-Rodriguez, A.M.; Vlček, Jr., A.; Unno, T.; Koike, K. *Inorg. Chem.*, **2007**, *46*, 3531-3540.
16. Vlček, Jr., A.; Farrell, I.R.; Liard, D.J.; Matousek, P.; Towrie, M.; Parker, A.W.; Grills, D.C.; George, M.W. *Dalton Trans.*, **2002**, 701-712.
17. (a) Cowan, A.J.; George, M.W. *Coord. Chem. Rev.*, **2008**, *252*, 2504-2511. (b) Lawes, D.J.; Geftakis S.; Ball, G.E. *J. Am. Chem. Soc.*, **2005**, *127*, 4134-4135. (c) Calladine, J.A.; Duckett, S.B.; George, M.W.; Matthews, S.L.; Perutz, R.N.; Torres, O.; Vuong, K.Q. *J. Am. Chem. Soc.*, **2011**.

133, 2303–2310. (d) Ball, G. E.; Brookes, C.M.; Cowan, A.J.; Darwish, T.A.; George, M.W.; Kawanami, H.K.; Portius, P.; Rourke, J.P. *Proc. Nat. Sci. USA*, **2007**, *104*, 6927-6932. (e) Duckett, S.B.; George, M.W.; Jina, O.S.; Matthews, S.L.; Perutz, R.N.; Sun, X.-Z.; Vuong, K.Q. *Chem. Commun.*, **2009**, *11*, 1401-1403. (f) Calladine, J.A.; Torres, O.; Anstey, M.; Ball, G.E.; Bergman, R.G.; Curley, J.; Duckett, S.B.; George, M.W.; Gilson, A.I.; Lawes, D.J.; Perutz, R.N.; Sun, X.-Z.; Vollhardt, K.P.C. *Chem. Sci.*, **2010**, *1*, 622-630.

18. Frisch, M.J.; Trucks, G.W.; Schlegel, H. B.; Scuseria, G. E.; Robb, M. A.; Cheeseman, J. R.; Zakrzewski, V. G.; Montgomery, J. A.; Stratmann, R. E.; Burant, J. C.; Dapprich, S.; Millam, J. M.; Daniels, A. D.; Kudin, K. N.; Strain, M. C.; Farkas, O.; Tomasi, J.; Barone, V.; Cossi, M.; Cammi, R.; Mennucci, B.; Pomelli, C.; Adamo, C.; Clifford, S.; Ochterski, J.; Petersson, G. A.; Ayala, P. Y.; Cui, Q.; Morokuma, K.; Malick, D. K.; Rabuck, A. D.; Raghavachari, K.; Foresman, J. B.; Cioslowski, J.; Ortiz, J. V.; Stefanov, B. B.; Liu, G.; Liashenko, A.; Piskorz, P.; Komaromi, I.; Gomperts, G.; Martin, R. L.; Fox, D. J.; Keith, T.; Al-Laham, M. A.; Peng, C. Y.; Nanayakkara, A.; Gonzalez, C.; Challacombe, M.; Gill, P. M. W.; Johnson, B. G.; Chen, W.; Wong, M. W.; Andres, J. L.; Head-Gordon, M.; Replogle, E. S.; Pople, J. A. *Gaussian 03 ReVision D. 01*; Gaussian, Inc., Wallingford CT, 2004.
19. Cooper A.I.; Poliakoff, M. *Chem. Phys. Lett.*, **1993**, *212*, 611-616.
20. Alamiry, A.H.; Boyle, N.M.; Brookes, C.C.; George, M.W.; Long, C.; Portius, P.; Pryce, M.T.; Ronayne, K.L.; Sun, X.-Z.; Towrie, M.; Vuong, K.Q. *Organometallics*, **2009**, *28*, 1461-1468.

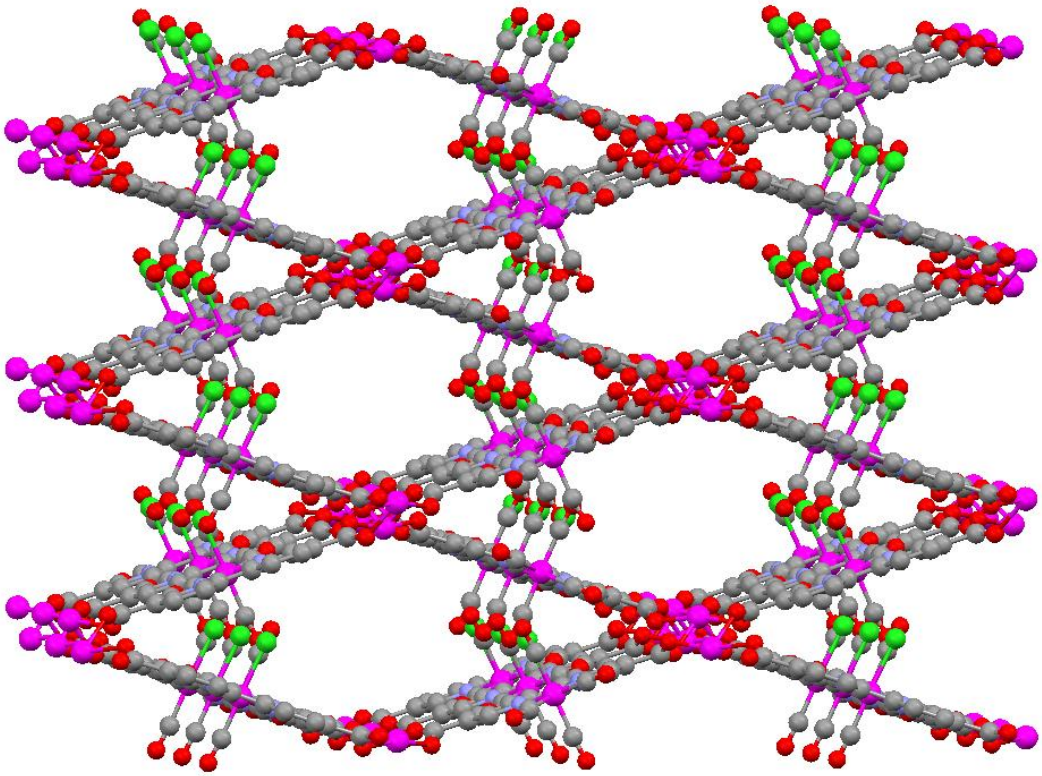

Figure 1 View of the three-dimensional framework structure of **ReMn** showing the interlinking of $[Mn(carboxylate]_{\infty}$ chains by $[Re(diimine)(CO)_3Cl]$ moieties.

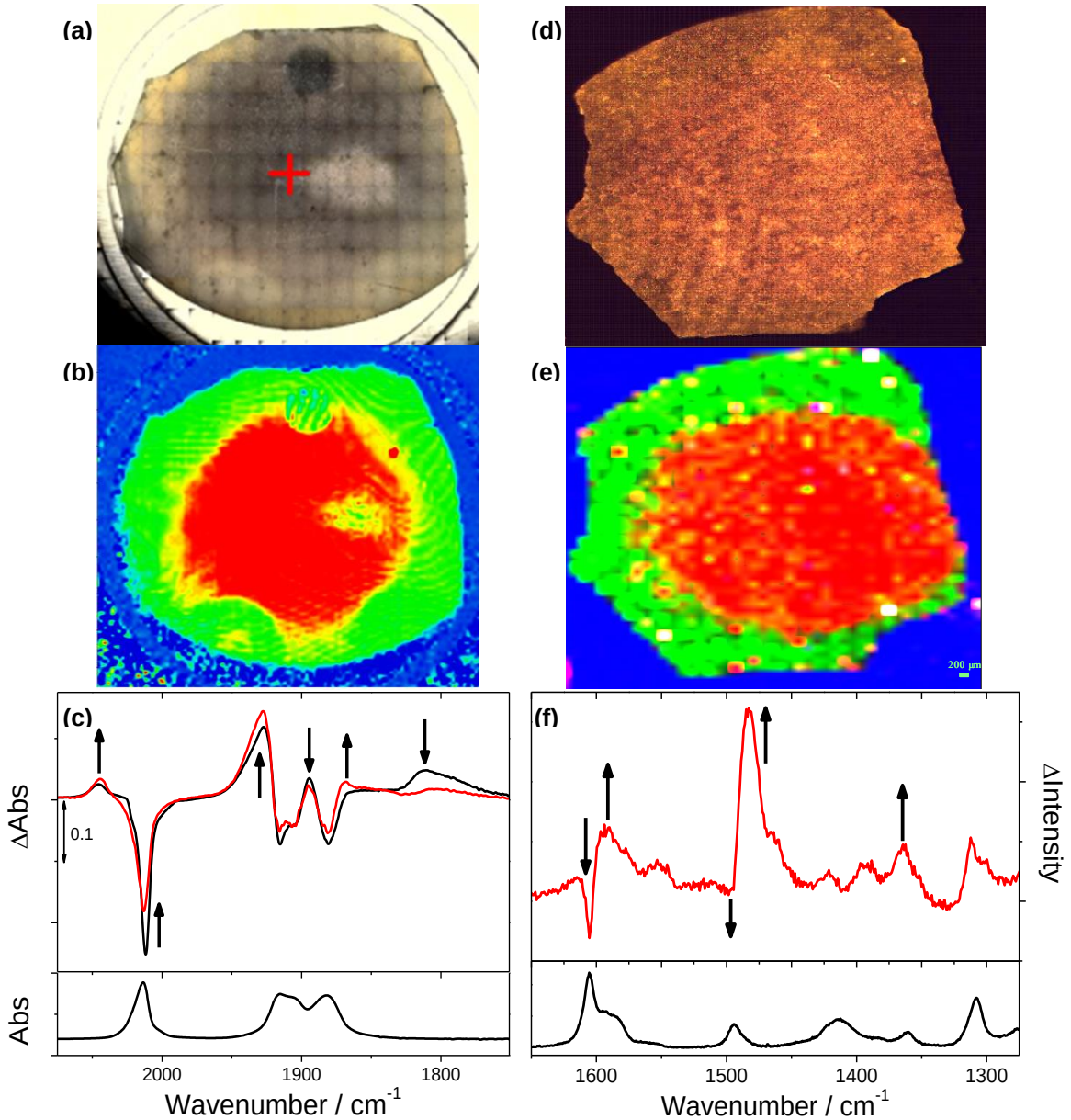

Figure 2 The results of separate FTIR and Raman mapping experiments of **ReMn** incorporated into KBr discs, post-UV photolysis. **(a)** The optical image and **(b)** FTIR image of the same KBr disc showing the ratio of the *mer*-isomer to the *fac*-isomer of **ReMn**. The red area shows the presence of *mer*-isomer, the green area the presence of *fac*-isomer and the blue area is where there is no KBr disc present. **(c)** The IR difference spectrum of **ReMn** in KBr after UV photolysis at 275 K, 200 s after photolysis (black line) and 10,000 s after photolysis. **(d)** The optical and **(e)** Raman image of another disc showing the regions corresponding to the presence of the *mer*-isomer (red) and the *fac*-isomer (green). The blue area is where no KBr disc is present. **(f)** The Raman difference spectrum at room temperature after UV photolysis recorded in an area where *mer*-isomer formation had occurred. (Figure (a)-(c) are reproduced with permission from reference 14.)

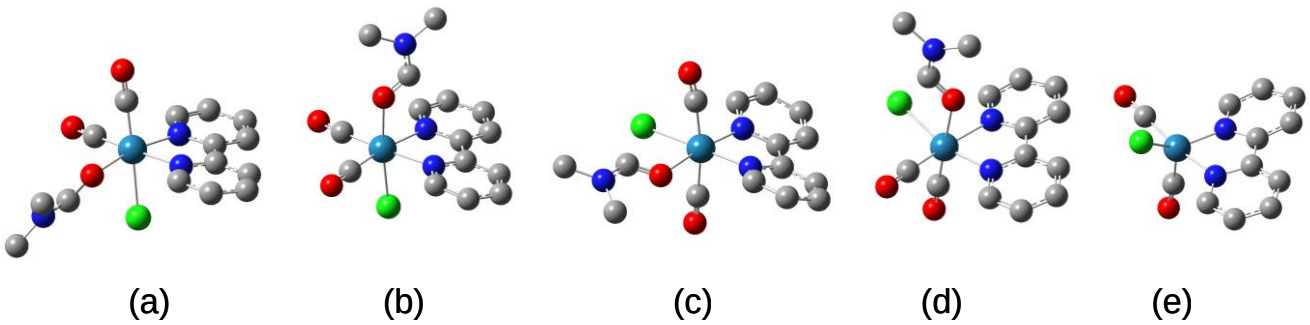

Figure 3 Possible structures (a – e, see text) of the dicarbonyl species [Re(bpy)$(CO)_2$Cl(L)] (where L = DMF or vacant site) calculated using DFT. (Hydrogens have been omitted for clarity).

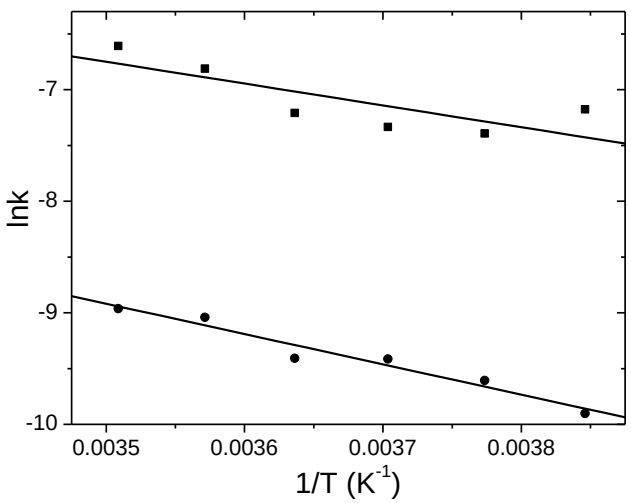

Figure 4 A plot of lnk *vs*. 1/T for the fast decay (*squares*) and the slow decay (*circles*) of the 1810 cm^{-1} band, showing linear fits to the data (*solid lines*).

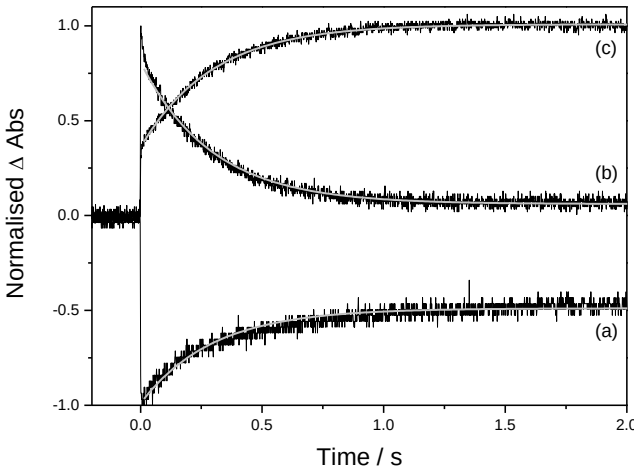

Figure 5 Kinetic traces obtained after 266 nm irradiation of *fac*-Re(dnb)$(CO)_3Cl$ in cyclopentane at room temperature, in the presence of 2 atm CO. Showing (a) partial recovery of the parent (1926 cm^{-1}); (b) decay of the dicarbonyl (1914 cm^{-1}) and (c) growth of the *mer*-isomer (1938 cm^{-1}).

Table 1 IR ν(CO) band positions of the *fac*- and *mer*-isomers and dicarbonyl intermediates of the [Re(diimine)$(CO)_n$Cl] (n = 2, 3) complexes in the MOF, in solution and as calculated (gas phase).

	***fac*-isomer ν(CO) IR bands**	**Dicarbonyl ν(CO) IR bands**	***mer*-isomer ν(CO) IR bands**
ReMn in KBr disc	2015, 1917, 1882	1893, 1855, 1813, 1794	2043, 1925, 1868
[Re(dnb)$(CO)_3$Cl] in:			
DMF	2018, 1912, 1889		
Cyclopentane + 10% DMF under Ar	2018, 1916, 1898	1905, 1882, 1814, 1802	Not observed.
Cyclopentane + 10% DMF under CO	2018, 1916, 1896	[a]1907, [a]1883, 1814, 1804	[b]2040, 1926, 1884
Cyclopentane under Ar and CO	2022, 1925, 1906	1922, 1915, 1902 1838, 1829, 1818	2045, 1937, 1894
Calculations[c]:			
[Re(bpy)$(CO)_3$Cl]	2100, 2028, 2006		2120, 2037, 1998
[Re(bpy)$(CO)_2$Cl] + vacant site		2070, 2028	
[Re(bpy)$(CO)_2$Cl] + CH_4-1 [d]		2019, 1967	
[Re(bpy)$(CO)_2$Cl] + CH_4-2 [d]		2022, 1960	
[Re(bpy)$(CO)_2$Cl] + CH_4-3 [d]		[e]	
[Re(bpy)$(CO)_2$Cl] + CH_4-4 [d]		2090, 2004	
[Re(bpy)$(CO)_2$Cl] + DMF-1 [d]		2004, 1955	
[Re(bpy)$(CO)_2$Cl] + DMF-2 [d]		1999, 1943	
[Re(bpy)$(CO)_2$Cl] + DMF-3 [d]		2010, 1951	
[Re(bpy)$(CO)_2$Cl] + DMF-4 [d]		2076, 1977	

[a] Uncertain band position. [b] Fitted from late-time FTIR spectrum after dicarbonyl species have decayed. [c] All frequencies are unscaled. [d] Number denotes position of adduct, see Scheme. [e] Does not optimise.

Table of Contents Entry

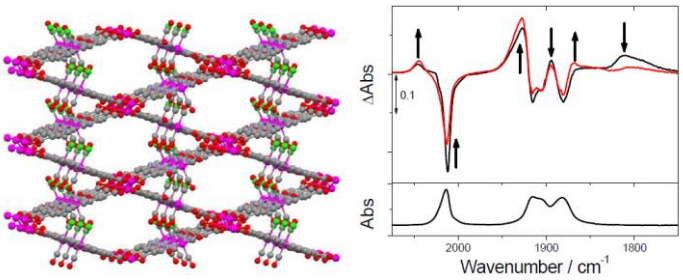

The mechanism and intermediates in the photo-initiated isomerization of *fac*-Re(diimine)$(CO)_3$Cl species incorporated into a 3D metal-organic framework (MOF) are reported. The *fac-mer* conversion is found to proceed via a dicarbonyl intermediate which undergoes transient binding to a DMF molecule.